van der Waals theory on the supercooled liquids of inverse-power potentials

Shaw Kambayashi
Tokai Research Establishment, Japan Atomic Energy Research Institute, Tokai, Naka, Ibaraki 319-11, Japan

Yasuaki Hiwatari
Department of Physics, Faculty of Science, Kanazawa University, Kanazawa, Ishikawa 920, Japan
(Received 31 July 1987)

By solving a self-consistent integral equation numerically, we have obtained the equations-of-state and thermodynamic properties of equilibrium supercooled liquids with soft-sphere potentials plus the Kac potential (generalized van der Waals model). The equations of state obtained deviate from those of molecular-dynamics simulations below the liquid-glass transition predicted. The static pair structures differ significantly along two branches, i.e., molecular-dynamics glasses and equilibrium supercooled liquids. From entropy curves obtained from the solutions of integral equations, we indicate the stability limit of the equilibrium supercooled liquid for the softness parameter $n=4$, 6, 9, 12, and ∞. We also discuss the effect of the softness on the thermodynamic properties of supercooled liquids.

I. INTRODUCTION

The equations of state of high-density or low-temperature liquids can be obtained through either integral equations based on the theory of liquids or computer simulations. Analytical or numerical solutions of integral equations usually must be accompanied by some approximations, without which the equations are impossible to solve.[1] On the other hand, computer simulations, either Monte Carlo or molecular-dynamics (MD) simulations, yield numerically exact solutions. This is, however, not the case in the metastable or glassy states, in which the relaxation time to attain an equilibrium state is much longer than the time scale of computer simulations.[2,3] With computer simulations of rapid quenching of liquids, one may prepare samples which are structurally arrested and which are far from equilibrium. Therefore, the resultant properties (structures, and so on) depend on the rate of quenching and the routes of it. On the other hand, the integral equation assuming homogeneity and equilibrium of the system yields the solutions of the most stable state which can exist in a supercooled regime. Such a state may be realized in laboratory experiments when the liquid is quenched as infinitely slowly as possible so that the liquid can always keep its equilibrium. Therefore, two approaches, namely, the integral equations and computer simulations, correspond to different limit cases, namely, infinitely slow quenching for the former and extremely fast quenching for the latter.

It is well known that the classical Percus-Yevick (PY) and hypernetted-chain (HNC) equations suffer from internal thermodynamic inconsistency, which can be overcome by a number of improvement schemes.[4–7] One of the most successful is the interpolation scheme of Rogers and Young (RY), which has the merit of being easily generalized to the case of mixtures.[8,9] Bernu *et al.* have found that the equation of state obtained by the RY integral equation for binary soft-sphere mixtures agrees very well with the molecular-dynamics data at temperatures above the liquid-glass transition.[8] The solutions of the thermodynamically self-consistent RY integral equation yield convincing theoretical evidence for the simultaneous existence of quenched amorphous (molecular dynamics) and fully relaxed equilibrium "fluid" states.

In this paper we present the solutions of the RY integral equation for one-component soft-sphere supercooled liquids interacting through inverse power potentials, $v(r)=\varepsilon(\sigma/r)^n$, where the softness parameter n is varied as $n=4$, 6, 9, 12, and ∞. We discuss n-dependent properties of thermodynamic functions, pair structure, and so on, in the supercooled liquid regime. In order to take into account attractions between atoms, we use the Kac potential. Thus our total potential between atoms is composed of the soft-sphere potential plus the Kac potential, which we called a generalized van der Waals model in our previous papers.[10,11] This model works very well for liquefied inert gases ($n=15$), liquid alkali metals ($n=4$), and some more complex liquids. Liquids are classified into groups, within this model, each of which takes a different n.

The solutions of the RY integral equation for our model yield a very simple equation of state which holds over the entire region of the supercooled liquids. Including an effect of the attractions by the Kac potential, we have calculated various thermodynamic functions, such as specific volume, compressibilities, enthalpies, entropies, and so on, as a function of temperatures at a constant pressure P, which we took $P=0$ for simplicity.

The equation of state for the crystalline state is easily obtained by using the Madelung constant and assuming an approximation of harmonic vibrations of atoms which hold exactly at low temperatures. Thus we can compare the thermodynamic functions of equilibrium supercooled liquids with those of crystalline states, at the

same temperature and pressure for each n. The resultant entropy curves show a cross point for all n which we investigated, indicating the stability limit of supercooled liquids, because the entropy of liquids must be larger than that of a crystalline solid at the same temperature and pressure. Such a stability limit of supercooled liquids is found to be located at a much lower temperature than a liquid-glass transition T_g predicted by molecular-dynamics simulations.

The pair structures obtained from the RY integral equations differ significantly from MD simulations in the glassy states. The former yields no splitting of the second peak, while the latter shows a clear splitting of the second peak below the glass transition. We will then investigate the temperature dependence of the ratio of the first maximum and the first minimum of the pair distribution function, which is called the Wendt-Abraham ratio, and of the half width at half maximum (HWHM) of the pair distribution function. With these analyses, we show that a characteristic property at the stability limit of the supercooled liquid is that the HWHM of the pair distribution function takes nearly a universal constant at the stability limit point, independent of the softness of the potentials.

II. THE MODEL

We consider a simple model liquid in which the atoms interact with pairwise additive purely repulsive inverse power pair potentials,

$$v(r)=\varepsilon\left[\frac{\sigma}{r}\right]^n , \tag{2.1}$$

where n (≥ 3) is the softness parameter of the potential. The case $n=\infty$ corresponds to a hard-sphere potential with core diameter σ. In our calculations, the integral equation was solved for the softness parameter $n=4$, 6, 9, 12, and ∞. The advantage of simple inverse power potentials is their scaling property. According to this property, all reduced equilibrium properties in excess of their ideal-gas counterparts depend only on one coupling parameter, not on the temperature and the number density separately. We take the following expression for this coupling parameter:[12,13]

$$\Gamma=\rho\sigma^3\left[\frac{k_BT}{\varepsilon}\right]^{-3/n} , \tag{2.2}$$

where ρ is the number density, k_B is the Boltzmann constant, and T is the temperature. For a hard sphere, Γ is reduced to $\rho\sigma^3$, but we use another parameter $\bar{\rho}$,

$$\bar{\rho}=\rho\sigma^3/\sqrt{2} , \tag{2.3}$$

i.e., the ratio of ρ and the fcc close-packing number density. The freezing points of inverse power potentials with $n=4$, 6, 9, 12, and ∞ are calculated by Hoover *et al.* with Monte Carlo simulations, and found to be $\Gamma=5.54$, 2.18, 1.33, 1.15, and $\bar{\rho}=0.667$ for $n=4$, 6, 9, 12, and ∞, respectively.[12–14]

The inverse power potential works very well for high-density liquids in which short-range repulsive force is dominant, but the pure repulsive potential leads to an unphysically high pressure. In order to investigate thermodynamic and structural properties at a more realistic condition, we have taken into account the effect of attractive interactions within the standard van der Waals mean-field approximation.[15] This approximation becomes exact in the limit of infinitely weak and long-range attractive potentials of the Kac form,[16]

$$w(r)=-a\gamma^3\exp(-\gamma r) , \tag{2.4}$$

where $\gamma\rightarrow 0$; the Helmholtz free energy can be obtained by adding a correction term to the free energy of inverse power potentials,[10]

$$F=F_0-\frac{4\pi a}{\rho} , \tag{2.5}$$

where F_0 is the free energy for $a=0$. From this equation, all zero-pressure thermodynamic and structural quantities can be calculated as functions of temperature. The freezing points for $a\neq 0$ slightly shift from that of the pure repulsive potential ($a=0$), but we may ignore such a small correction for the location of the freezing point.

Equation (2.5) is useful because in this model the repulsive force and attractive force can be treated separately. This model has been found to work for various liquids by choosing a suitable softness of inverse power potentials; for example, the case $n=15$ corresponds to liquefied inert gases and the case $n=4$ corresponds to liquid alkali metals.[10] From Eq. (2.5), once we know the thermodynamic properties for $a=0$, we can obtain those for $a\neq 0$. Note that the Kac potential, Eq. (2.4), gives no influence on the properties of the structures (both static and dynamic).

III. ROGERS-YOUNG INTEGRAL EQUATION

A. Integral equation

Equilibrium distribution functions allow a complete but compact description of microscopic structure of liquids, as well as provide a quantitative measure of the correlations between the positions of different particles. Furthermore, knowledge of the lowest-order distribution function is generally sufficient to calculate most equilibrium properties of the system. In particular, if the molecules of the system interact with pairwise additive central force, knowledge of the pair distribution function allows the calculation of the excess internal energy U^{ex}, equation of state $P\beta/\rho$, and the compressibility χ_T,[1]

$$\frac{U^{ex}}{N}=2\pi\rho\int g(r)v(r)r^2dr , \tag{3.1}$$

$$\frac{P\beta}{\rho}=1-\tfrac{2}{3}\pi\beta\rho\int g(r)r^3\frac{dv(r)}{dr}dr , \tag{3.2}$$

$$\rho k_BT\chi_T=1+4\pi\rho\int[g(r)-1]r^2dr , \tag{3.3}$$

where $g(r)$ is the pair distribution function and N the total number of atoms.

Integral equations of the equilibrium theory of liquids have been used to calculate the pair distribution function.[1] These integral equations result from the combination of two relations. The first one, which is exact, is the Ornstein-Zernike relation between the pair correlation function $h(r)=g(r)-1$ and the direct correlation function $c(r)$,

$$h(r)-c(r)=\rho\int h(r')c(|\mathbf{r}-\mathbf{r}'|)d\mathbf{r}' . \tag{3.4}$$

The second one is an approximation closure between these functions, examples of which are given by the Percus-Yevick and hypernetted-chain closures, respectively,

$$g(r)=\exp[-\beta v(r)][1+\gamma(r)] , \tag{3.5}$$

$$g(r)=\exp[-\beta v(r)+\gamma(r)] , \tag{3.6}$$

where $\gamma(r)=h(r)-c(r)$ is the sum of the nodal diagrams. The classic integral equation, like the PY and HNC equations, suffers from internal thermodynamical inconsistency. The "thermodynamical consistency" means the consistency for the equations of state obtained from three different results, i.e., Eqs. (3.1), (3.2), and (3.3). For pure repulsive potentials, the PY and HNC equations of state bracket the "exact" computer simulation results.[6] This suggests that some interpolation of the two equations would overcome the inconsistency, and a number of improvement schemes were investigated. The integral equation introduced by Rogers and Young, which has been used here, is one of the most successful schemes, and its thermodynamic and structural results for the inverse power potential well agree with the computer simulation results in a liquid regime.[7] In this integral equation, PY and HNC closures are interpolated by a function which depends on the interparticle distance,

$$g(r)=\exp[-\beta v(r)]\left[1+\frac{\exp[f(r)\gamma(r)]-1}{f(r)}\right] , \tag{3.7}$$

where $f(r)$ is the "mixing function" $(0\le f\le 1)$. In general, the mixing function must contain two parameters to achieve thermodynamical consistency, but for the simple soft-sphere model only one parameter is required because the equations of state which are calculated from Eqs. (3.1) and (3.2) are identical. So the mixing function is conveniently taken in the form[10]

$$f(r)=1-\exp(-\alpha r) , \tag{3.8}$$

where $\alpha>0$ is a mixing parameter. Note that in this scheme the integral equation is reduced to PY closure at $r=0$ and HNC closure at $r=\infty$. Equations (3.4), (3.7), and (3.8) together make it possible to achieve thermodynamic consistency.

With the exception of the PY approximation for the hard sphere, it is possible to solve the integral equation only numerically. The method for solving the RY integral equation used here is some modification of iterative procedure given by Ng.[17] In it, the direct correlation function is chosen to input and output functions. For a given input function $c^{\text{in}}(r)$, the Fourier transform $\hat{c}(k)$ is calculated and using Ornstein-Zernike relation, Eq. (3.4), the Fourier transform of $\hat{\gamma}(k)$ is determined. $\gamma(r)$ then follows from an inverse Fourier transformation and $c^{\text{out}}(r)$ is obtained from RY closure, Eq. (3.7). The superscripts in and out mean the input and output functions, respectively. Using the output functions thus obtained as the next input function, a number of iterations were made so that the self-consistent measure Δ is minimized,

$$\Delta=\left[\int |c^{\text{in}}(r)-c^{\text{out}}(r)|^2 r^2 dr\right]^{1/2} . \tag{3.9}$$

It took about 100 iterations at a large coupling constant Γ to obtain a self-consistent measure Δ less than 5×10^{-10}, which is small enough to ensure the validity of the solutions.

The mixing parameter α used in the above calculation as a trial was tested as follows. There are two methods to adjust it. First, the inverse compressibility $\beta/(\rho\chi_T)$ obtained from Eq. (3.3) is integrated step by step from $\Gamma'=\Gamma_0$ to $\Gamma'=\Gamma$ and the resulting pressure is compared with the virial pressure calculated from Eq. (3.2) at $\Gamma'=\Gamma$. Second, virial pressure is numerically differentiated at a given Γ and compared with the $\beta/(\rho\chi_T)$ by Eq. (3.3).[1] We have used the second method for our starting low coupling state ($\Gamma'=\Gamma_0$), and in successive calculations for higher coupling states the first method was used. Thermodynamic consistency was ensured within 0.01% in our calculations. The parameter α thus determined is listed in Table I at the freezing point. Our values are very close to the value calculated by Rogers and Young. Rogers and Young stressed that the mixing parameter does not depend on the coupling constant in the liquid region. Our results show that this is almost valid, but in the supercooled regime α systematically decreases, as plotted in Fig. 1.

To solve the integral equation, we used a dimensionless length $x=r/l$, where $l=\rho^{-1/3}$ for soft spheres and $l=\sigma$ for hard spheres. The grid points and step size were chosen as 2048 points and $\Delta x=0.01$, respectively, and the fast-Fourier-transform routine was used in iterations.

B. Solution

The solution of the RY integral equation yields the pair distribution function, equation of state, and isothermal compressibility. Figure 2 plots the pair distribu-

TABLE I. The value of the mixing parameter α in the RY integral equation at the freezing point for various softness n's. The values in parentheses are the results by Rogers and Young (Ref. 7).

n	$\alpha^*=\alpha l$
4	1.585 (1.794)
6	1.192 (1.209)
9	0.792 (0.804)
12	0.593 (0.603)
∞	0.279 (0.251)

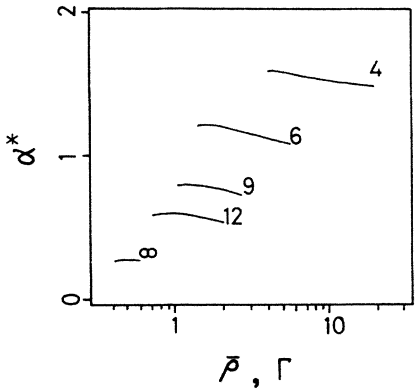

FIG. 1. Coupling dependence of the consistency parameter α for various softness ($n=4$, 6, 9, 12, and ∞).

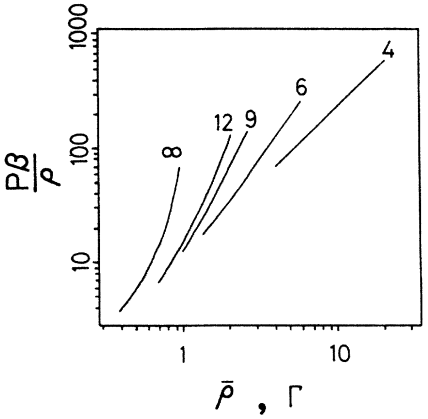

FIG. 3. Equation of state by RY solutions.

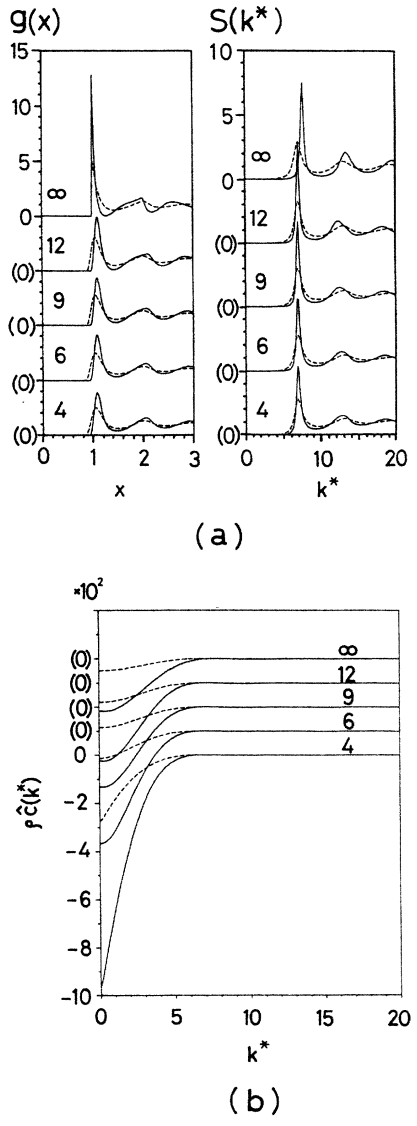

FIG. 2. Structural properties of inverse power systems at the freezing point (dashed curves) and the stability limit (solid curves). (a) Pair distribution function $g(x)$ and structure factor $S(k^*)$. (b) Fourier transform of the direct correlation function $\hat{c}(k^*)$.

tion functions $g(x)$, structure factors $S(k^*)$ ($k^*=kl$), and the Fourier transform of direct correlation functions $\hat{c}(k^*)$ at the freezing point and stability-limit point which will be discussed in greater detail in Sec. IV. Comparison of the RY pair distribution functions with those of the computer simulations for $n=12$ reveals that both results are in an excellent agreement for Γ less than about 1.5, at which the computer simulated samples are transformed into a glassy state; the RY pair distribution function does not show a splitting of the second peak for all Γ's, unlike the computer simulated samples which do for $\Gamma \gtrsim 1.5$.[18,19] We note the RY $g(x)$ is a pair distribution function of equilibrium supercooled states which are different from the computer generated states obtained by a fast quenching, i.e., structurally arrested glasses.

The equations of state of the inverse power systems are plotted in Fig. 3. In Fig. 4 the molecular-dynamics results for $n=12$ are compared with the RY solutions.[20] The linear behavior of the equation of state versus Γ^4 is easily understood from a simple model of harmonic vi-

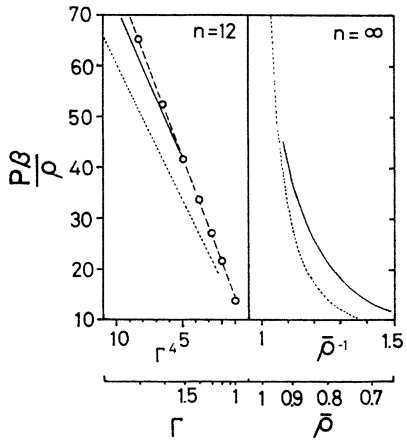

FIG. 4. Equation of state for $n=12$ and ∞. Solid curves are the present RY solutions, dotted curves represent the crystalline solid state. For the 12th inverse power system, the molecular-dynamics results are shown by the dashed curve with open circles.

brations of atoms of high-density or low-temperature solid states. With this model we calculated the equation of state of a crystalline solid. The excess internal energy can be written in the following form:

$$\frac{U^{ex}}{N}=b\varepsilon(\rho\sigma^3)^{n/3}+\tfrac{3}{2}k_BT+O(T^2)\ , \tag{3.10}$$

where b is a Madelung constant which determines the zero-pressure lattice energy.[22] The corresponding equation of state leads to

$$\frac{P\beta}{\rho}-1=\frac{n}{2}+\frac{n}{3}b\Gamma^{n/3}\ . \tag{3.11}$$

For the fcc lattice structure, $b=7.981$, 3.613, 2.208, and 1.516 for $n=4$, 6, 9, and 12, respectively.[22] The equation of state of the supercooled liquid and glassy states is very well fitted by Eq. (3.11) with a larger b than that of a crystalline solid (see Table II). Figure 4 also shows that for the 12th-inverse power potential the RY solution and molecular-dynamics results show an excellent agreement in the supercooled liquid range up to $\Gamma\sim1.5$. Beyond that coupling constant a clear bifurcation is observed; the RY results drop progressively below the MD data as Γ increases. A similar behavior has been reported for soft-sphere mixtures.[8] This trend could be attributed to a gradual breakdown of the RY closure under very-strong-coupling conditions, but this does not seem to be very likely since different implementations of the thermodynamic self-consistency requirement lead to nearly identical results, as shown in Ref. 8. We believe that the different pressures correspond to two physically different branches of the equation of state. The upper branch obtained by molecular dynamics may be associated with typical glassy states, i.e., a quenched nonequilibrium state which we were unable to relax within the duration of the simulation, since the structural relaxation times increase by many orders of magnitude beyond the glass transition ("structural arrest"). This branch is of course not unique and may depend, among other factors, on the cooling rate during the preparation of the initial configuration of the samples. Also, the point beyond which bifurcation occurs may depend on the initial preparation. The lower branch, the solution of the RY integral equation, however, corresponds to an ideal metastable disordered state of the lowest free energy, since the integral equation assumes a translationally invariant equilibrium which would be reached after a sufficiently long structural relaxation process. True thermodynamic equilibrium can only be reached by translational symmetry-breaking nucleation into the crystal phase which is characterized by significantly lower pressures, as shown in Fig. 4. For the hard-sphere model, the above simple model for the crystalline solid state makes no sense. Then, the equation of state of hard spheres in the solid phase is calculated from free-volume theory,[23]

$$\frac{P\beta}{\rho}=1+(\bar{\rho}^{-1/3}-1)^{-1}\ . \tag{3.12}$$

Equation (3.12) is plotted in Fig. 4 together with RY results.

TABLE II. The "Madelung constant" of RY supercooled liquids and crystalline solids.

n	RY supercooled liquid	Crystalline solid
4	8.102	7.981
6	3.689	3.613
9	2.298	2.209
12	1.655	1.516

IV. GENERALIZED van der WAALS MODEL

A. The stability limit

The bifurcation of the equation of state and the ensuing difference in slopes beyond the glass transition are reminiscent of the distinct "kinks" in a number of thermodynamic properties with temperatures at constant pressure observed in many simulations of a one-component system.[19,24–26] The inverse power potential under investigation leads to unphysically high pressure due to its purely repulsive nature of interaction forces. In order to investigate thermodynamic properties at zero pressure, we have taken into account the effect of attractive interactions within the standard van der Waals mean-field approximation. This approximation becomes exact in the limit of infinitely weak and long-range attractive potentials of the Kac form given by Eq. (2.4). In the following we make a simplifying assumption that $a=\varepsilon\sigma^3$, where ε is the same energy scale as in Eq. (2.1). Therefore, the resulting equation of state takes a simple form of the van der Waals type,[10,15]

$$\frac{P\beta}{\rho}=P_0^*(\Gamma)-4\pi\Gamma(T^*)^{-(n-3)/n}\ , \tag{4.1}$$

where $P_0^*(\Gamma)$ is the equation of state for the inverse power potential. Hereafter, the 0 index is attached to the system of the inverse power potentials. The condition of zero pressure yields then the following simple relation between the coupling constant Γ and temperature T^*:

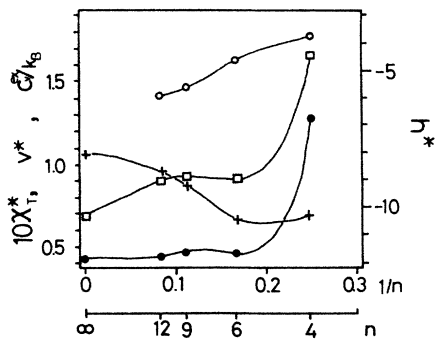

FIG. 5. Softness (n) dependence of various thermodynamic properties at the freezing point.

$$T^* = \left[\frac{P_0^*(\Gamma)}{4\pi\Gamma} \right]^{-n/(n-3)} . \quad (4.2)$$

With the RY solution of the equation of state $P_0^*(\Gamma)$ and isothermal compressibility $\overline{\chi_T^0} = \rho\chi_T^0/\beta$ and Eq. (4.2), all zero-pressure thermodynamic quantities can be calculated as a function of the reduced temperature T^*. For such quantities we have calculated the reduced volume per particle (specific volume) v^*, the excess specific heat c_v^{ex} at constant volume, reduced compressibility $\chi_T^* = \chi_T \varepsilon/\sigma^3$, the reduced enthalpy per particle h^*, and entropy per particle S^*:

$$v^* = \frac{1}{\rho\sigma^3} = \frac{(T^*)^{-3/n}}{\Gamma} , \quad (4.3)$$

$$c_v^{ex}/k_B = \frac{3}{n}\left[\frac{n+3}{n} P_0^*(\Gamma) - \frac{3}{n}(\overline{\chi_T^0})^{-1} - 1 \right] , \quad (4.4)$$

$$(\chi_T^*)^{-1} = \rho\sigma^3 T^* (\overline{\chi_T^0})^{-1} - 8\pi(\rho\sigma^3)^2 , \quad (4.5)$$

$$h^* = \frac{U+PV}{N} , \quad (4.6)$$

$$S^* = \frac{S}{Nk_B} = \frac{U\beta}{N} - \frac{F\beta}{N} , \quad (4.7)$$

where F is the Helmholtz free energy. These quantities for $n=4$, 6, 9, 12, and ∞ at the corresponding freezing point are plotted in Fig. 5. The softness (n) dependence of the compressibility and enthalpy is significant. The temperature dependence of specific volume v^* is plotted in Fig. 6 with molecular-dynamics results for $n=12$. It is of interest to note that the RY results present nearly linear properties for a wide temperature range, which is in a marked contrast to the MD results at low temperatures.

For each n, the entropy curves of the RY supercooled liquids and crystalline solid show a clear cross point (see Fig. 7). This point indicates the stability limit of the supercooled liquid because the entropy of liquids must be larger than that of crystalline solids at the same temperature and pressure. The coupling constant at the stability limit thus obtained is listed in Table III, being significantly larger than the liquid-glass transition predicted by molecular-dynamics simulations. The glass transition may depend on the quenching rate and the initial conditions of the sample. It is well known that the slower the quenching rate, the larger the expected glass transition. The quenching rate used in MD simulations is an order of $\sim 10^{12}$–10^{10} deg/sec, which is much faster than that of laboratory experiment. Therefore, the glass transition obtained by MD simulations may be considered to be an upper limit of the liquid-glass transition, while laboratory experiments using a much slower quenching rate may yield the liquid-glass transition situated between the MD glass transition and the stability limit shown in Table III.

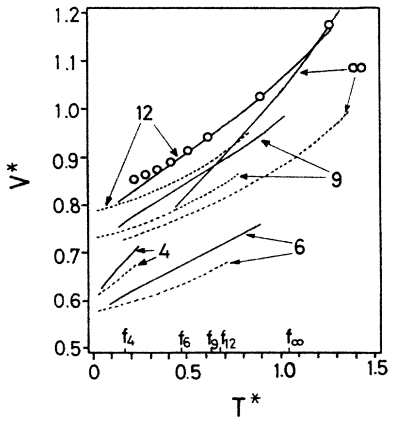

FIG. 6. Temperature dependence of the specific volume for various softness parameters. f_n indicates the freezing point for the softness parameter n. The symbols are the same as in Fig. 4.

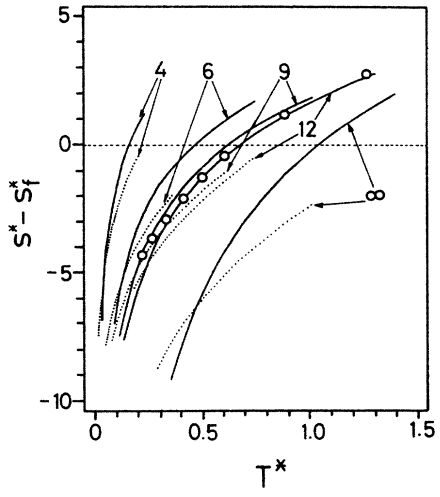

FIG. 7. Temperature dependence of entropy per particle in excess of that at the freezing point for various softness parameters. The symbols are the same as in Fig. 4.

B. Structural properties near the stability limit

For the study of the characteristic structural properties near the stability limit we have examined the so-called Wendt-Abraham ratio R (the ratio between the first maximum and the first minimum of the pair distri-

TABLE III. The range of the liquid-glass transition of inverse power systems. The glass transition couplings of the 12th inverse power system and hard-sphere model are taken from Ref. 8 and 21, respectively.

n	Freezing point	Glass transition	Stability limit
4	$\Gamma=5.54$		15.01
6	2.18		4.46
9	1.33		2.30
12	1.15	1.56	1.72
∞	$\bar{\rho}=0.667$	0.806	0.870

bution function),[27] half width at half maximum of the pair distribution function, and the coordination number Nc,

$$Nc = 4\pi\rho \int_0^{r_m} g(r) r^2 dr \ , \tag{4.8}$$

where r_m is the position of the first minimum of the pair distribution function.

It has been pointed out that the empirical Wendt-Abraham ratio is reflected by a quenching rate; for the 12-6 Lennard-Jones (LJ) system the ratio is 0.14 by Monte Carlo simulation and 0.09 by molecular-dynamics simulation at the liquid-glass transition (the quench rate in the Monte Carlo method is presumably much larger than that in the molecular-dynamics method).[25–27] For the 12th-inverse power system, R is 0.08 at the liquid-glass transition.[28] We have calculated the Wendt-Abraham ratio at the stability limit of inverse power supercooled liquids obtained by the RY integral equation [see Fig. 8(b)]. It is found that for the softness $n=12$, near the glass transition, the RY solution shows a significantly smaller R than the molecular-dynamics result.

It is evident that the RY solution is a characteristic of fully relaxed disordered structures corresponding to an infinitely slow quenching rate. The temperature dependence of R was obtained so as to be linear, as that of the specific volume shown in Fig. 6.

In Fig. 8(a), the W_{HWHM}/r_1 at the freezing point and stability limit is shown (where r_1 is the position of the first peak of the pair distribution function). In solid states the HWHM gives an order of magnitude of the root-mean-square displacement of atoms. It is seen in this figure that $W_{\mathrm{HWHM}}/r_1 \simeq 0.1-0.15$ at the melting point, while $W_{\mathrm{HWHM}}/r_1 \simeq 0.08$ at the stability limit. The softness dependence of the HWHM at the stability limit is very weak, indicating that the W_{HWHM}/r_1 at the stability limit is an almost universal constant, independent of the type of pair interactions.

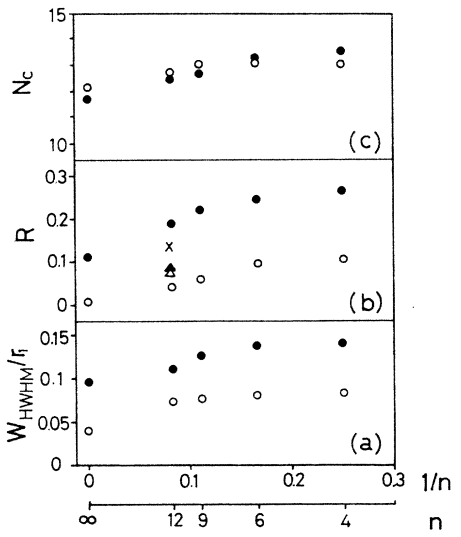

FIG. 8. Softness (n) dependence of (a) W_{HWHM}/r_1 of $g(r)$, (b) Wendt-Abraham ratio R, and (c) coordination number N_c at the freezing point (●) and stability limit (○). Points marked by ×, ▲, and △ are those obtained from Monte Carlo simulation for the Lennard-Jones system, molecular-dynamics simulation for the LJ system and for the inverse power system with $n=12$, respectively, at the liquid-glass transition (Refs. 27, 25, and 28).

The coordination number calculated from Eq. (4.8), i.e., the population of the first shell (near-neighbor atoms surrounding an atom), is plotted in Fig. 8(c). The temperature dependence is weak below the freezing point. All these values are between 12 and 13, and are comparable to those of computer glasses.[28] Therefore, the packing order is quite similar for all states below the freezing point.

V. DISCUSSION

We have studied the thermodynamic properties and pair distribution functions of the generalized van der Waals supercooled liquids based on the Rogers-Young integral equation of fluid theory. The RY solution yields the same equation of state as the molecular-dynamics result up to the coupling constant Γ, less than the glass transition Γ_g predicted by the molecular-dynamics simulations. Below T_g the equation of state obtained from the RY equation deviates from that of MD simulations. Glasses are nonequilibrium states in nature, and the structural relaxation time of glasses is many orders of magnitude larger than that of equilibrium liquids. The equation of state in glasses may depend on the quenching rate, the route of it, and initial configurations. The solution of the thermodynamically self-consistent RY integral equation yields the equation of state for fully relaxed "fluid" states, which may be obtained by quenching a liquid at an infinitely slow cooling rate. Therefore, the present results yield convincing theoretical evidence for the simultaneous existence of quenched amorphous and fully relaxed fluid states. The fluid branch plays a physically important role as an underlying limit state for the glassy state obtained by molecular-dynamics simulations or by laboratory experiments (relatively large cooling rates).

The second point of the present results is the n (softness) dependence of the thermodynamic and structural properties of the supercooled liquid. Among them, it has been found that the HWHM predicts an almost universal constant at the stability-limit point, irrespective of the value of n, except the hard-sphere potential ($n=\infty$). The HWHM is a measure of a root-mean-square displacement of atoms in solid states. Therefore, the above result gives an empirical law for the order of magnitudes of the vibrations of atoms at the stability-limit point of supercooled liquids.

ACKNOWLEDGMENTS

Part of this work was supported by a Grant-in-Aid for Scientific Research. One of us (Y.H.) is grateful to Professor J. P. Hansen for valuable discussions. Our computations were carried out on FACOM M-360 at the Computer Center of Kanazawa University.

[1]J. P. Hansen and I. R. McDonald, *Theory of Simple Liquids*, 2nd ed. (Academic, London, 1987).
[2]E. Leutheusser, Phys. Rev. A **29**, 2765 (1984).
[3]J. J. Ullo and S. Yip, Phys. Rev. Lett. **54**, 1509 (1985).
[4]Y. Rosenfeld and N. V. Ashcroft, Phys. Rev. A **20**, 1208 (1979).
[5]P. Hutchinson and W. R. Conkie, Mol. Phys. **24**, 567 (1972).
[6]D. S. Hall and W. R. Conkie, Mol. Phys. **40**, 907 (1980).
[7]F. J. Rogers and D. A. Young, Phys. Rev. A **30**, 999 (1984).
[8]B. Bernu, J. P. Hansen, Y. Hiwatari, and G. Pastore (to be published).
[9]J. P. Hansen and G. Zerah, Phys. Lett. A **108**, 277 (1985).
[10]Y. Hiwatari and H. Matsuda, Prog. Theor. Phys. **47**, 741 (1972).
[11]H. Matsuda and Y. Hiwatari, in *Cooperative Phenomena*, edited by H. Haken and M. Wagner (Springer-Verlag, Berlin, 1973).
[12]W. G. Hoover, S. G. Gray, K. W. Johnson, D. Henderson, J. A. Barker, and B. C. Brown, J. Chem. Phys. **52**, 4931 (1970).
[13]W. G. Hoover, S. G. Gray, and K. W. Johnson, J. Chem. Phys. **55**, 1128 (1971).
[14]J. P. Hansen, Phys. Rev. A **2**, 221 (1970).
[15]J. L. Lebowitz and O. Penrose, J. Math. Phys. **7**, 98 (1966).
[16]M. Kac, Phys. Fluid **2**, 8 (1959); M. Kac, G. E. Uhlenbeck, and P. C. Hemmer, J. Math. Phys. **4**, 216 (1963).
[17]K. C. Ng, J. Chem. Phys. **61**, 2680 (1974).
[18]Y. Hiwatari, J. Phys. Soc. Jpn. **47**, 733 (1979).
[19]W. D. Kristensen, J. Non-Cryst. Solids **21**, 303 (1976).
[20]S. Kambayashi and Y. Hiwatari, J. Phys. Soc. Jpn. **56**, 2788 (1987).
[21]J. M. Gordon, J. H. Gibbs, and P. D. Fleming, J. Chem. Phys. **65**, 2771 (1976).
[22]J. O. Hirschfelder, C. F. Curtiss, and R. B. Bird, *Molecular Theory of Gases and Liquids* (Wiley, New York, 1954).
[23]R. J. Buehler, R. H. Wentorf, J. O. Hirschfelder, and C. F. Curtiss, J. Chem. Phys. **19**, 61 (1951).
[24]J. H. R. Clarke, J. Chem. Soc. Faraday Trans. 2 **75**, 1371 (1979).
[25]S. Nose and F. Yonezawa, Solid State Commun. **56**, 1005 (1985).
[26]M. Kimura and F. Yonezawa, in *Topological Disorder in Condensed Matter*, edited by F. Yonezawa and T. Ninomiya (Springer-Verlag, Berlin, 1983).
[27]H. R. Wendt and F. F. Abraham, Phys. Rev. Lett. **41**, 1244 (1978).
[28]Y. Hiwatari, J. Phys. C **13**, 5899 (1980).